Supplemental figure 1

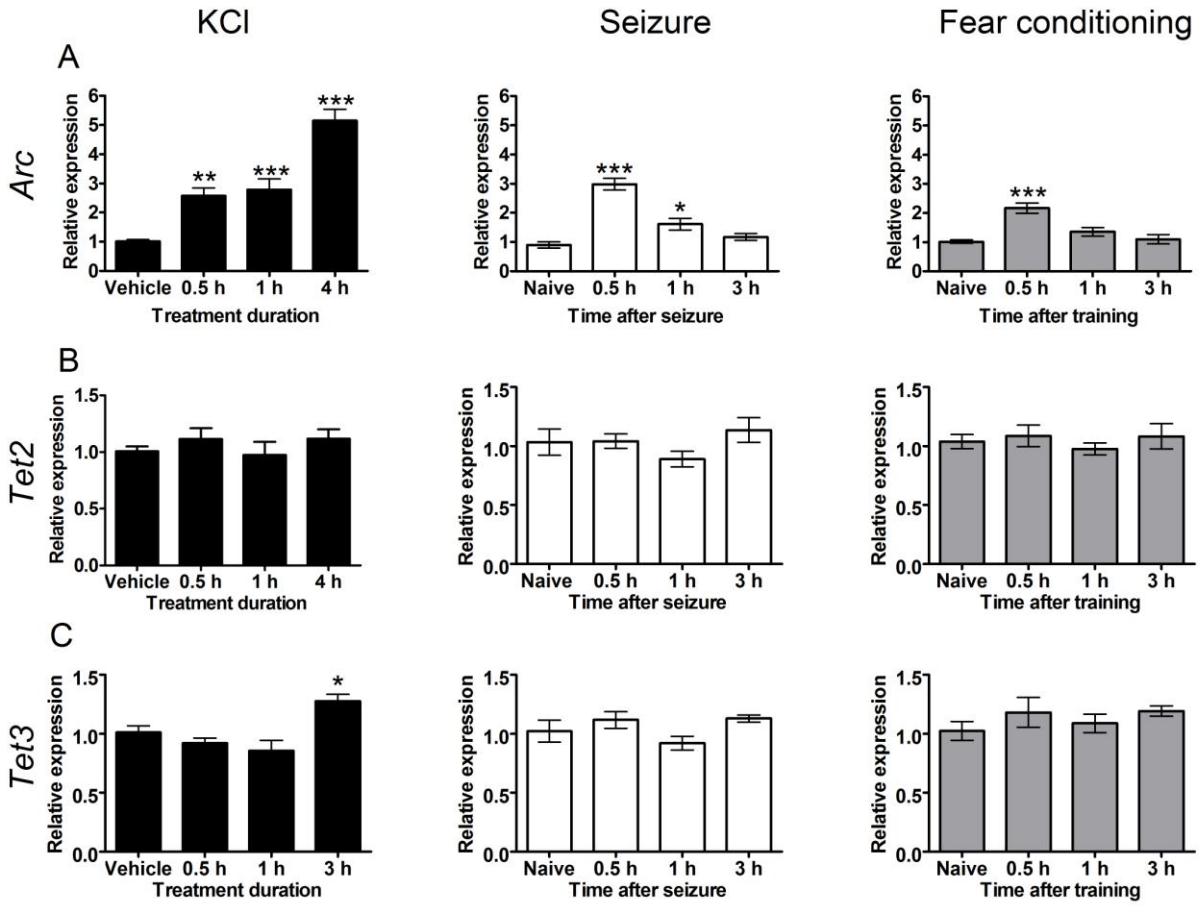

Figure S1. Expression levels of *Arc*, *Tet2* and *Tet3* following neuronal activation *in vitro* and *in vivo.* Quantitative reverse-transcription PCR (qRT-PCR) analysis of gene expression in primary hippocampal neuron cultures depolarized with 25 mM KCl (black bars), *in vivo* after flurothyl-induced seizure (white bars) and following contextual fear conditioning (grey bars). (A) Relative *Arc* expression. KCl ($F_{3, 21}$ = 45.70); seizure ($F_{3, 25}$ = 33.27); fear conditioning ($F_{3, 35}$ = 13.70). Either vehicle versus KCl treatment or naives versus experienced animals. *p < 0.05, **p < 0.01, ***p < 0.001; one-way ANOVA followed by Bonferroni *post hoc* test. (B) Relative *Tet2* expression. KCl treatment, ($F_{3, 21}$ = 0.89); seizure, ($F_{3, 25}$ = 1.18); fear conditioning ($F_{3, 35}$ = 0.42). p > 0.05, one-way ANOVA followed by Bonferroni *post hoc* test. (C) Relative *Tet3* expression. KCl treatment, ($F_{3, 21}$ =

7.15); seizure ($F_{3, 25}$ = 2.13); fear conditioning versus naive ($F_{3, 35}$ = 0.86). *p < 0.05, one-way ANOVA followed by Bonferroni *post hoc* test. Data are the combination of 2-3 independent experiments. KCl treatment (*n* = 4-9/group), seizure (*n* = 6-7/group), fear conditioning (*n* = 9). All data are presented as mean ± s.e.m.

Supplemental figure 2

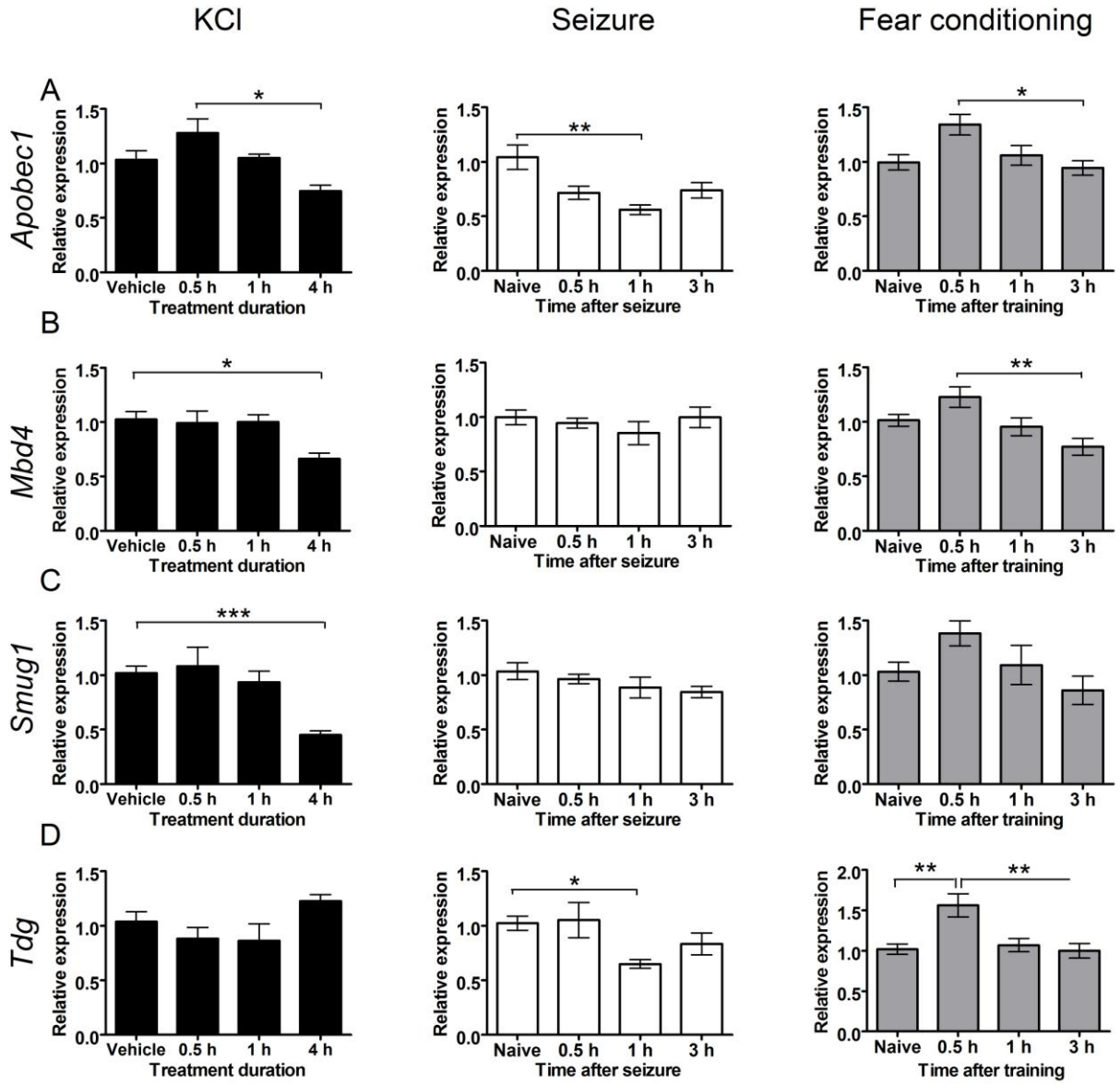

Figure S2. Expression levels of *Apobec1, Mbd4, Smug1 and Tdg* following neuronal activation *in vitro* and *in vivo.* Quantitative reverse-transcription PCR (qRT-PCR) analysis of gene expression in primary hippocampal neuron cultures depolarized with 25 mM KCl (black bars), *in vivo* after flurothyl-induced seizure (white bars) and following contextual fear conditioning (grey bars). (A) Relative *Apobec1* expression. KCl ($F_{3, 24}$ = 3.90); seizure ($F_{3, 29}$ = 5.86); fear conditioning

($F_{3, 32}$ = 4.92). *p < 0.05, **p < 0.01; one-way ANOVA followed by Bonferroni *post hoc* test. (B) Relative *Mbd4* expression. KCl treatment, ($F_{3, 24}$ = 3.70); seizure, ($F_{3, 29}$ = 0.65); fear conditioning ($F_{3, 32}$ = 5.78). *p < 0.05, **p < 0.01; one-way ANOVA followed by Bonferroni *post hoc* test. (C) Relative *Smug1* expression. KCl treatment, ($F_{3, 24}$ = 8.85); seizure ($F_{3, 29}$ = 1.44); fear conditioning ($F_{3, 32}$ = 2.56). ***p < 0.001, one-way ANOVA followed by Bonferroni *post hoc* test. (D) Relative *Tdg* expression. KCl treatment, ($F_{3, 24}$ = 1.75); seizure ($F_{3, 29}$ = 3.61); fear conditioning ($F_{3, 32}$ = 7.28). *p < 0.05, **p < 0.01; one-way ANOVA followed by Bonferroni *post hoc* test. . Data are the combination of 2-3 independent experiments. KCl treatment (*n* = 4-12/group), seizure (*n* = 6-11/group), fear conditioning (*n* = 7-10/group). All data are presented as mean ± s.e.m.

Supplemental figure 3

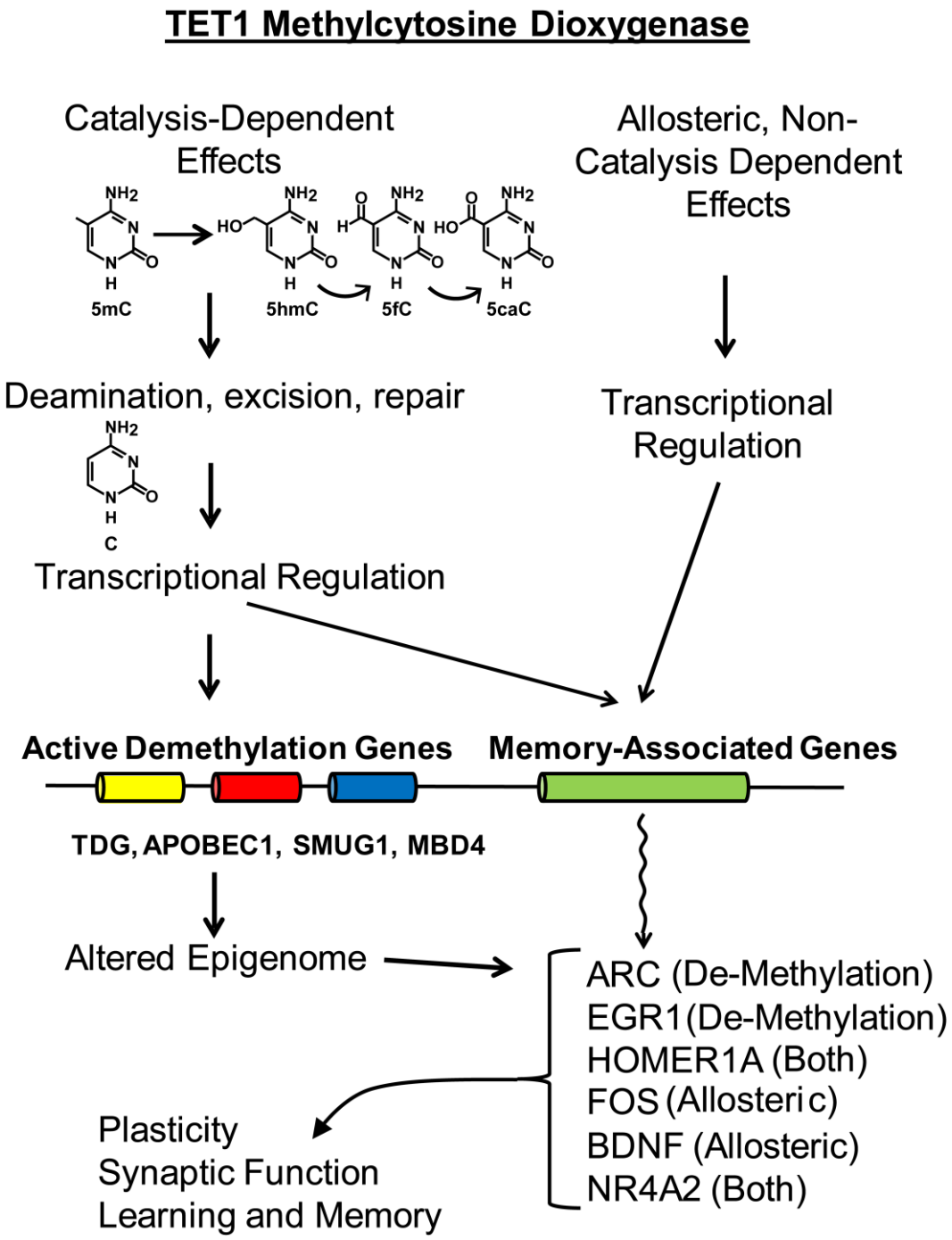

Figure S3. Roles of TET1 in CNS epigenetic and transcriptional regulation. TET1 is involved in multiple pathways controlling both active demethylation via methylcytosine oxidation (left-hand

pathway) and non-enzymatically mediated allosteric regulation of transcriptional activation (right-hand pathway). Both pathways are likely involved in overall control of the capacity for memory formation in the adult CNS. It is important to note that the two pathways can act in concert, that is, the two delineated roles of TET1 are not mutually exclusive. The upstream mechanisms regulating these two major pathways remain mysterious at this time. In addition, the full extent of genes epigenetically targeted by TET1 is not known and either positive or negative dysregulation of a variety of memory genes we did not investigate could also contribute to the disruption of memory we observed.

Table S1. List of primers used in this study

Gene	Sense primer (5'->3')	Antisense primer (5'->3')	Tm used for qRT-PCR
Hprt1	GGAGTCCTGTTGATGTTGCCAGTA	GGGACGCAGCAACTGACATTTCTA	60
Gapdh	GTGGAGTCATACTGGAACATGTAG	AATGGTGAAGGTCGGTGTG	60
Gusb	CAGACTCAGTTGTTGTCACCT	TCAACTTCAGGTTCCCAGTG	60
Tbp	CCAGAACTGAAAATCAACGCAG	TGTATCTACCGTGAATCTTGGC	60
Rpl13a	ATGTCCCCTCTACCCACAG	TGAACCCAATAAAGACTGTTTGC	60
Tet1	GAGCCTGTTCCTCGATGTGG	CAAACCCACCTGAGGCTGTT	60
Tet2	TGTTGTTGTCAGGGTGAGAATC	TCAACTTCAGGTTCCCAGTG	60
Tet3	CCGGATTGAGAAGGTCATCTAC	AAGATAACAATCACGGCGTTCT	60
Bdnf (total)	CACAGACGGCTCCTGCCAATTTAT	TTTCTGATGCTCAGGAACCCAGGA	**62**
Arc	ACGATCTGGCTTCCTCATTCTGCT	AGGTTCCCTCAGCATCTCTGCTTT	60
Ppp1 gamma	TTGCTTGCTTTGTGATCATACC	GAGACCCTCATGTGTTCCTTC	60
c-Fos	AATGGTGAAGACCGTGTCAGGA	TTGATCTGTCTCCGCTTGGAGTGT	60
Calcineurin B	AAGATGGGAAATGAGGCGAG	CTCAGGCAGAGACATGAACTC	60
Reelin	AGTACTCAGATGTGCAGTGGGCAA	AGCGCTCCTTCAGGAAAGTCTTCA	60
Homer1a	TGCAAAGGAGAAGTCGCAGGAGAA	CATGATTGCTGAATTGAATGTGTACCT	60
Glur1	TCCGTATGGCTTCATTGATGG	ATCGAGTTCTGCTACAAATCCC	60
Cdk5	TCCCCATTCCTGTTTATGAGC	CTGGACCCTGAGATTGTGAAG	60
CamKIIa	CTGGTTCAAAGGCTGTCATTC	CTGATCGAAGCCATAAGCAATG	60
Egr1	AGCGCCTTCAATCCTCAAG	TTTGGCTGGGATAACTCGTC	60
Tdg	CGATCCTGTGCTAATCTCTGG	TGCTGTTCTGTCACGGTTG	60
Apobec1	ACCTGAGGAAACAAAGTCCG	GAGTGGGATCAACAGCTACAG	60
Smug1	GGAGCCACACCGTAACTATG	AACACATTCACTTCCCCAAAG	60
Mbd4	GAAGCAGCAGGTGAAGCAAATCGT	TGGGCATTTCAGAGCCATCCTGTA	60
Ppp1 beta	GCGAGTTTGACAATGCTGGTGGTA	ACGTCCAGAATTCAGCCCACCATA	60
PP2A alpha	GCTGCAATCATGGAACTTGAC	GGTTCATGGCAATACTGTACAAG	60
Nr4a2	AGCCACCTTGCTTGTACCAAATGC	TTGTAGTAAACCGACCCGCTGTGT	60

Supplemental Experimental Procedures

Primary Neuronal Culture

Hippocampi from C57BL/6-background P0-P2 mouse brains were dissected in HBSS (Gibco), digested in papain (Worthington), washed with Neurobasal-A medium supplemented with L-glutamine and B27 (Gibco), and dissociated with fire-polished glass pipettes in the same medium. The cell suspension was passed through a 70 μm filter and centrifuged. Cells were resuspended in medium and seeded on poly-L-lysine-coated (Sigma) 12-well plates (Corning). One half of the medium was replaced at 4 DIV, and the experiment was performed at 6 DIV.

Flurothyl seizure induction

Seizures were induced by placing mice individually in a 2.8 L closed plastic chamber. Flurothyl (2,2,2-trifluroethyl ether, Sigma-Aldrich) was administered by infusion (20 uL/min) using a 1 mL syringe driven by an infusion pump (KD Scientific Model 200) onto filter paper suspended at the top of the chamber. Upon visual evidence of Tonic-clonic seizures (defined as whole body clonus followed by running and bouncing) animals were immediately removed from the chamber and allowed to recover.

Western Blotting

Crude protein lysates were generated by homogenizing hippocampal tissue in 2X sample buffer containing a 1X concentration of Halt Protease and Phosphatase Inhibitor Cocktail (Pierce) and centrifuged for 10 min at 10,000 x g at 4^{o}C. The supernatant was used for immunobloting. Equal amounts of total protein (25 μg) were loaded in each protein lane of SDS-PAGE and, after electrophoresis; proteins were transferred onto PVDF membrane and double probed with rabbit anti-HA tag antibody (Abcam, ab9110) at a 1:3000 dilution and Mouse anti-Actin (Abcam, ab3280) at a 1:2000 dilution in 0.1% TBS-T at room temperature (RT) for 2 h. This was followed by incubation with Li-COR IRDye 680 Goat anti-Rabbit (Li-COR, 926-68071) and Li-COR IRDye

800CW Goat anti-Mouse (Li-COR, 926-32210) at a 1:15,000 dilution in 0.1% TBS-T for 1 hour. Membranes were imaged using an Odyssey Imager (LI-COR).

Hippocampal tissue dissection

Isolation of hippocampal area CA1 from whole brain was preformed as previously described (Miller and Sweatt, 2007). Brains were submerged in oxygenated (95%/5% O2/CO2) ice-cold cutting solution (125 mM NaCl, 3 mM KCl, 1.25 mM NaH2PO4, 25 mM NaHCO3, 0.5 mM CaCl2, 7 mM MgCl2, 10 mM glucose, 0.6mM ascorbate) immediately after rapid decapitation and removal of the brain. Sequential coronal sections dorsal hippocampi were generated using a scalpel. In each coronal section area CA1 was gently separated from DG from using a 30 gauge needle and a Needle Blade Microsurgical Knife (Fine Science Tools). Only the top third of CA1 containing the Stratum pyramidale was retained for experimentation, which could be visualized prior to removal, with the assistance of a fiber optic illuminator (Cole-Palmer Instrument Company). All dissections were carried out under a dissecting scope and immediately frozen on dry ice and stored at -80^{o}C until further processing. For virus-transfected tissue, CA1 was dissected under UV light using a Nikon SMZ1500 stereomicroscope.

RNA extraction and qRT-PCR

RNA was extracted using the RNeasy Mini Kit (Qiagen) according to the manufacturer's instructions and was eluted in 30 ul of RNase-free water. 150 ng of total RNA was converted to cDNA using the iSrcipt cDNA synthesis Kit (Bio-Rad). Quantitative reverse transcriptase PCR was performed on an iQ5 real-time PCR detection system using iQ™ SYBR® Green Supermix and 300 μM of primer. All qRT-PCR primers were designed using Primer Quest (Integrated DNA Technologies) to span exon-exon junctions or were acquired directly as pre-designed PrimeTime® qPCR Primer Assays (Integrated DNA Technologies) (Table S1). For all RT-PCR data, hypoxanthine guanine phosphoribosyl transferase (Hprt1) was used as an internal control. The comparative Ct method was used to calculate differences in gene expression between samples (Livak and Schmittgen, 2001; Pfaffl, 2001).

DNA extraction and hydrolysis

DNA was extracted from tissues using a QIAamp DNA micro kit (Qiagen) according to the manufacturer's instructions and eluted in 50ul of buffer AE. DNA hydrolysis was performed using DNA degradase Plus (Zymo Research). Briefly, 200ng of genomic DNA, measured using Quant-it dsDNA assay kit (Life Technologies), was diluted to 40ul with ddH20 and mixed with 5ul of 10X DNA Degradase Reaction Buffer, 0.75ul of DNA Degradase Plus and water to reach a total reaction volume of 50ul in 0.2ml PCR tubes. The reaction mixture was then incubated at 37oC for 3 hours in an iCycler Thermal Cycler (Bio-Rad).

MRM quantitation

10µL of DNA hydrolysis samples were diluted 1:5 with methanol containing 250 ng of digested DNA and injected onto a reverse phase liquid chromatography (HPLC) column (Atlantis dC18, 2.1 x 100mm, 3 µm particle size, Waters) equilibrated and eluted (0.1 mL/min) using a gradient increase of the organic buffer (100% methanol) from 1 to 60%, at a rate of 15%/min, for the elution of nucleosides. The aqueous buffer consisted of water/methanol/formic acid (95:5:0.1, v/v/v). The effluent from the column was directed into a waste collection container using a Valco divert valve for the first 0.5 minutes of each sample run to collect possible salts (harmful to mass spectrometer) and then the eluted nucleosides were diverted to an electrospray ion source connected to a triple quadrupole mass spectrometer (Applied Biosystems MDS Sciex API 5000) operating in the positive ion MRM mode using previously optimized conditions, and the intensities of specific MH+→ fragment ion transitions were recorded (5mC m/z 242.1+→126.1, 5hC m/z 258.1+→142.1, and deoxycytidine (dC) m/z 228.1+→112.1). The measured percentage of 5mC and 5hmC in each experimental sample was calculated from the MRM peak area divided by the combined peak areas for 5mC plus 5hmC plus C (total cytosine pool). With each batch of experimental samples, a series of standard samples was simultaneously prepared and analyzed using 897bp DNA standards containing C, 5mC or 5hmC, respectively (Zymo research). The standard samples contained

increasing amounts of 5mC and 5hmC in the presence of the same amount of C (0–10% for 5mC and 0–1% for 5hmC). Calibration curves were constructed for 5mC and 5hmC from the data obtained from the standard samples (measured 5mC or 5hmC peak area/total cytosine pool plotted against actual percentage of either 5mC or 5hmC in the samples). The measured percentage of 5mC and 5hmC in each experimental sample was then converted to actual percentage 5mC and 5hmC by interpolation from the calibration curves. This provided a correction for any differences that might exist in the molar MRM responses of the various nucleosides.

Statistical Analysis

Statistical comparisons between two groups were performed using an unpaired t-test. Statistical analysis between three or more groups was accomplished using One-way ANOVA with Bonferroni post test. All statistical analyses were performed using GraphPad Prism version 4.00 for Windows (GraphPad Software, San Diego California USA).

Supplemental references

Bekinschtein, P., Cammarota, M., Katche, C., Slipczuk, L., Rossato, J.I., Goldin, A., Izquierdo, I., and Medina, J.H. (2008). BDNF is essential to promote persistence of long-term memory storage. Proc Natl Acad Sci U S A 105, 2711-2716.

Chwang, W.B., Arthur, J.S., Schumacher, A., and Sweatt, J.D. (2007). The nuclear kinase mitogen- and stress-activated protein kinase 1 regulates hippocampal chromatin remodeling in memory formation. J Neurosci *27*, 12732-12742.

Datson, N.A., Meijer, L., Steenbergen, P.J., Morsink, M.C., van der Laan, S., Meijer, O.C., and de Kloet, E.R. (2004). Expression profiling in laser-microdissected hippocampal subregions in rat brain reveals large subregion-specific differences in expression. Eur J Neurosci 20, 2541-2554.

Globisch, D., Munzel, M., Muller, M., Michalakis, S., Wagner, M., Koch, S., Bruckl, T., Biel, M., and Carell, T. (2010). Tissue distribution of 5-hydroxymethylcytosine and search for active demethylation intermediates. PLoS One 5, e15367.

Guo, J.U., Su, Y., Zhong, C., Ming, G.L., and Song, H. (2011). Hydroxylation of 5-methylcytosine by TET1 promotes active DNA demethylation in the adult brain. Cell 145, 423-434.

James, A.B., Conway, A.M., and Morris, B.J. (2005). Genomic profiling of the neuronal target genes of the plasticity-related transcription factor -- Zif268. J Neurochem 95, 796-810.

Khare, T., Pai, S., Koncevicius, K., Pal, M., Kriukiene, E., Liutkeviciute, Z., Irimia, M., Jia, P., Ptak, C., Xia, M., et al. (2012). 5-hmC in the brain is abundant in synaptic genes and shows differences at the exon-intron boundary. Nat Struct Mol Biol 19, 1037-1043.

Le, T., Kim, K.P., Fan, G., and Faull, K.F. (2011). A sensitive mass spectrometry method for simultaneous quantification of DNA methylation and hydroxymethylation levels in biological samples. Anal Biochem 412, 203-209.

Livak, K.J., and Schmittgen, T.D. (2001). Analysis of relative gene expression data using real-time quantitative PCR and the 2(-Delta Delta C(T)) Method. Methods 25, 402-408

Miller-Delaney, S.F., Das, S., Sano, T., Jimenez-Mateos, E.M., Bryan, K., Buckley, P.G., Stallings, R.L., and Henshall, D.C. (2012). Differential DNA methylation patterns define status epilepticus and epileptic tolerance. J Neurosci 32, 1577-1588.

Mizuno, M., Yamada, K., Olariu, A., Nawa, H., and Nabeshima, T. (2000). Involvement of brain-derived neurotrophic factor in spatial memory formation and maintenance in a radial arm maze test in rats. J Neurosci 20, 7116-7121.

Nestor, C.E., Ottaviano, R., Reddington, J., Sproul, D., Reinhardt, D., Dunican, D., Katz, E., Dixon, J.M., Harrison, D.J., and Meehan, R.R. (2012). Tissue type is a major modifier of the 5-hydroxymethylcytosine content of human genes. Genome Res 22, 467-477

Oliveira, A.M., Hemstedt, T.J., and Bading, H. (2012). Rescue of aging-associated decline in Dnmt3a2 expression restores cognitive abilities. Nat Neurosci 15, 1111-1113.

Pfaffl, M.W. (2001). A new mathematical model for relative quantification in real-time RT-PCR. Nucleic Acids Res 29, e45.

Shen, L., Wu, H., Diep, D., Yamaguchi, S., D'Alessio, A.C., Fung, H.L., Zhang, K., and Zhang, Y. (2013). Genome-wide analysis reveals TET- and TDG-dependent 5-methylcytosine oxidation dynamics. Cell 153, 692-706.

Williams, K., Christensen, J., Pedersen, M.T., Johansen, J.V., Cloos, P.A., Rappsilber, J., and Helin, K. (2011). TET1 and hydroxymethylcytosine in transcription and DNA methylation fidelity. Nature 473, 343-348.

Zhang, L., Lu, X., Lu, J., Liang, H., Dai, Q., Xu, G.L., Luo, C., Jiang, H., and He, C. (2012). Thymine DNA glycosylase specifically recognizes 5-carboxylcytosine-modified DNA. Nat Chem Biol 8, 328-330.

Zhu, J.K. (2009). Active DNA demethylation mediated by DNA glycosylases. Annu Rev Genet 43, 143-166.